Journal of
Materials Chemistry B

Materials for biology and medicine

Accepted Manuscript

This article can be cited before page numbers have been issued, to do this please use: S. Alavi, K. Sokolowski, C. F. Dial, Z. P. Bulman and R. A. Gemeinhart, *J. Mater. Chem. B*, 2026, DOI: 10.1039/D5TB02919H.

ROYAL SOCIETY OF CHEMISTRY

rsc.li/materials-b

View Article Online
DOI: 10.1039/D5TB02919H

ARTICLE

Drug Delivery with Fewer Fouls: Localized Antibiotic Release and Reduced Surface Biofouling with Glutathione-conjugated Hydrogels

Submitted TBD

DOI: TBD

Sonia Alavi[a,†], *Karol Sokolowski*[a,†], *Catherine F. Dial*[a], *Zackery P. Bulman*[b], *and Richard A. Gemeinhart*[a,c,*]

Systemic antibiotics are the standard of care for acute bacterial skin and skin structure infections (ABSSSI), but low drug perfusion at the site of infection and higher rates of antibiotic resistance necessitates alternative strategies to enhance local antibiotic concentrations. Wound dressings provide a convenient approach to antibiotic delivery but are limited by fixed, pre-loaded antibiotic concentrations. We have recently demonstrated the use of glutathione-conjugated poly(ethylene glycol) [GSH-PEG] hydrogels for the loading and release of charge-bearing therapeutic molecules. Herein, we evaluate the antibacterial and antibiofilm activities of rationally selected therapeutics released from GSH-PEG hydrogels. Antibiotics release from GSH-PEG hydrogels inhibited the growth of *Pseudomonas aeruginosa* and *Staphylococcus aureus* and effectively reduced biofilm formation without significantly influencing hDFAs proliferation and migration. In addition to controlled antibiotic delivery, GSH-conjugated hydrogels demonstrated markedly lower albumin and bacterial adsorption as compared to unconjugated hydrogels and a traditional wound dressing. The zwitterionic GSH ligands within hydrogels permit selective therapeutic delivery while reducing biofouling, highlighting the GSH-PEG hydrogel platform as a promising candidate for use as a wound dressing material.

Introduction

Acute bacterial skin and skin structure infections (ABSSSI), also commonly referred to as skin and soft tissue infections (SSTIs), constitute a burdensome and costly concern for healthcare systems globally.[1-5] In the United States alone, SSTIs have been estimated to account for approximately 3% of all emergency department visits, or about 3.4 million cases annually, and contribute substantially to hospital admissions and healthcare utilization .[6, 7] Despite systemic antibiotic therapy, treatment failure rates in ABSSSI remain substantial, with recent multicenter studies reporting non-response in up to 19% of hospitalized patients and recurrence rates exceeding 25%, underscoring the ongoing clinical challenge these infections pose.[8, 9]

The observed rates of ABSSSI treatment failure and recurrence have been attributed to insufficient target site concentration, systemic toxicities, and the growing prevalence of antibiotic resistance.[1, 2, 10-13] Simply increasing systemic antibiotic dose or duration in an attempt to address poor antibiotic penetration to the infection has not been shown to improve outcomes.[14] Furthermore, such measures encounter dose-limiting toxicities, increased risk of infectious complications such as *Clostridium difficile*-associated diarrhea, and overall risk of adverse effects increasing by 5% for each day exceeding 8 days of therapy.[14-18] New approaches to antibiotic therapy through novel delivery schemes or antibiotic combinations may overcome biological hurdles, improve cure rates, and prevent recurrence.[19-21]

Direct application of antibiotics at the wound site, most often as a powder or irrigation solution, is a common practice employed by surgeons and physicians to prevent ABSSSIs.[22-24] However, clinical guidelines do not support the prevention or treatment of ABSSSIs with topical antibiotics as a result of the heterogeneous antibiotic distribution, absorption, and activity with the non-standardized approaches.[25, 26] In addition to serving as a platform for localized and controlled antimicrobial delivery, wound dressings can be designed to provide moisture retention, gas permeation, and a physical barrier to benefit ABSSSI wound resolution.[27-30] Unfortunately, wound dressings may also carry negative attributes such as supporting biofilm adherence and fouling by wound exudate components, resulting in prolonged infection and further trauma to the wound bed upon removal.[31, 32] Hydrogels have emerged as a favorable dressing material providing a hydrated matrix amendable to functionalization for localized drug delivery and minimizing unintentional impairment of the healing process.[27-29, 33, 34]

[a] *Department of Pharmaceutical Sciences, University of Illinois Chicago, Chicago, IL, USA*
[b] *Department of Pharmacy Practice, University of Illinois Chicago, Chicago, IL, USA*
[c] *Departments of Biomedical Engineering, and Ophthalmology and Visual Sciences, University of Illinois Chicago, Chicago, IL, USA*
* Corresponding author: rag@uic.edu
† co-first authors

Electronic Supplementary Information (ESI) available: Detailed description of the materials used and supplementary data to this article, specifically hDFA proliferation following exposure to free antibiotics, hDFA migration in the presence of hydrogels preincubated with protein, and bacterial isolate growth in the presence of non-drug loaded cotton gauze, PEG hydrogels, and GSH-PEG hydrogels. See DOI: 10.1039/TBD

DOI: 10.1039/D5TB02919H

Current wound dressings contain broad-spectrum inorganic antimicrobials, such as silver and iodine.[31, 32, 35, 36] While these agents remain convenient in treatment and prevention of ABSSSIs, concerns of local cytotoxicity and microbial resistance exist due to strict formulations that cannot be tailored to a patient's infection.[21, 37-39] Shelf stability, variable drug properties, and microbial resistance further pose significant barriers to developing clinically accessible dressings containing traditional antibiotic agents.[21, 35] As such, there is a clear need for novel dressing materials capable of flexible loading for safe, effective, and timely administration of antimicrobials within a clinical environment.

We recently described glutathione-conjugated poly(ethylene glycol) hydrogels (GSH-PEG) showing promise to address the limitations of existing wound dressing materials.[40, 41] In our previous report, we focused upon exploring the mechanisms governing the association within and subsequent release of charged drugs from GSH-PEG hydrogels.[42] Intended for anchoring recombinant GSH-S-transferase proteins, the GSH ligands demonstrated the ability to bind charge-bearing small molecules through electrostatic and hydrogen bonding.[40-42]

The PEG-conjugated, zwitterionic GSH ligands may also lead to reduced surface biofouling as materials bearing zwitterionic and anionic charges have demonstrated reduced protein biofouling onto polymeric dressing surfaces.[43-45] Thus, clinicians may be able to tailor each wound dressing to the patient's infection while considering the pathogen's susceptibility, the patient's allergies, and the surface area of the wound, among other factors. Building on our previous findings establishing GSH-PEG hydrogels as a local antibiotic delivery platform,[46] we investigated additional characteristics relevant to GSH-PEG hydrogels for localized antibiotic delivery when antibiotic resistance is encountered. Extending beyond localized drug delivery, a hydrogel intended for wound application must also function favorably at the tissue-material interface, where compatibility with host repair processes, biofilm persistence, and adsorption of wound-associated biological components can all shape therapeutic outcomes. In this context, the present work evaluates GSH-PEG hydrogels as a biomaterial at the wound interface. Specifically, we assessed dermal fibroblast proliferation and migration in the presence of GSH-PEG hydrogels as *in vitro* indicators of cytocompatibility, examined the activity of antibiotic-loaded GSH-PEG hydrogels against mature biofilms developed by clinically relevant Gram-positive and Gram-negative wound pathogens, and study protein, bacterial, and biofilm fouling at the hydrogel surface. Collectively, this study positions GSH-PEG hydrogels as a multifunctional platform for localized and personalized antibiotic delivery.

Experimental

Materials

Information regarding materials and bacterial isolates utilized are described in detail within the Supplemental Information (S.I.).

Hydrogel Polymerization

Hydrogels were polymerized as previously described.[40] Briefly, monomer solutions were prepared in deionized water, unless otherwise noted, containing 16% poly(ethylene glycol) diacrylate (PEGDA) (w/w) [Mn 575], 0.05% Irgacure® 2959 (w/v), and in the presence (GSH-PEG) or absence (PEG) of 60 mM GSH. The monomer solutions were then placed between two glass coverslips separated by plastic spacers (1.6 mm), polymerized under UV-light (0.75 mW/cm^2; measured on UVX radiometer), and subsequently cut using a 6-mm cork borer. GSH incorporation occurs during UV-initiated polymerization through thiol-mediated reaction of the GSH thiol with PEGDA acrylate groups, yielding pendant GSH moieties within the hydrogel network.[42,47] All hydrogels were washed for a minimum of three days in deionized water with at least one solution change per day unless otherwise specified. Sterilization of hydrogels was performed UV exposure for 30 minutes total, 15 minutes on each side, prior to use in bacterial and hDFA bioassays.

Susceptibility Testing of Bacterial Isolates

Bacterial isolates, *Pseudomonas aeruginosa* [ATCC27853, AR0514, AR0440, AR0459, AR0441, CNP23] and *Staphylococcus aureus* [ATCC29213, ATCC33591, AR0479, AR0565, AR0219, AR0220], were maintained at -80°C in cation-adjusted Mueller–Hinton broth (CAMHB) with 20% glycerol and were subcultured twice on tryptic soy agar plates supplemented with 5% sheep blood prior to use. Stock antibiotic solutions of each agent were freshly prepared as single-use aliquots at the beginning of each week and kept frozen at -80°C. Minimum inhibitory concentrations (MIC) were measured in triplicate by broth microdilution according to Clinical and Laboratory Standards Institute (CLSI) guidelines.[48] *Escherichia coli* (*E. coli)* ATCC 25922 and *S. aureus* ATCC 29213 were utilized as quality control organisms. Modal MIC values are reported.

Drug Diffusion

Agar-well drug diffusion bioassays were conducted as previously described.[42] Briefly, bacterial isolates were prepared as suspensions in Dulbecco's phosphate-buffered saline (DPBS) to a 1.0 McFarland standard, approximately 1 x 10^8 colony forming units (CFU)/mL, subsequently lawned onto the surface of a cation-adjusted Mueller–Hinton agar plate, and allowed to dry for 10 minutes. A 6-mm cork borer was then used to create a well in the center of the agar plate into which the loaded hydrogel (40.8 ± 1.3 µL) was placed. Sterilized hydrogels were loaded with or without drug in PBS (vancomycin [32 mg/mL], meropenem [16 mg/mL], or amikacin [50 mg/mL] at the limit of solubility) for 1 hour and briefly washed for 15 minutes in DPBS prior to use.[42] Plates were incubated for 24 hours in ambient air at 35°C after which the diameter of inhibitory zones was measured using a ruler.[48] No observable bacterial growth inhibition received a diameter value of 6 mm; equivalent to the GSH-PEG hydrogel diameter value. Approximation of 24-hour drug release for vancomycin and meropenem can be found in the human dermal fibroblasts (hDFA) proliferation subsection below.

View Article Online
DOI: 10.1039/D5TB02019K

Cell Culture Maintenance

Primary hDFA cells were thawed and maintained within a humidified 37°C incubator with 5% CO_2 in Dulbecco's modified Eagle's medium (DMEM) supplemented with 5% fetal bovine serum (FBS) and 1% penicillin-streptomycin. Culture media was changed every 3 days with cell passaging occurring upon reaching approximately 80% confluence.[49] For all experiments outlined below, cells were utilized between passages 4-6 and incubated in DMEM supplemented with 5% FBS within a humidified 37°C incubator with 5% CO_2 unless otherwise noted.

hDFA Proliferation

Cells were seeded at a density of 5,000 cells per well in a 96-well plate and allowed to adhere over a period of 24 hours. Concurrently, sterilized hydrogels were loaded with or without the drug in DMEM (vancomycin [32 mg/mL] or meropenem [16 mg/mL]) for 1 hour. Following loading, hydrogels were briefly washed for 15 minutes in DPBS prior to placement into 2 mL of DMEM with 5% FBS for 24 hours, intended to serve as a reference point for downstream bacterial time-kill analyses.[19, 20, 50] The conditioned DMEM was sterile-filtered prior to use. Following hDFA adherence, cells were washed twice with 200 µL DPBS prior to the application of 100 µL conditioned media, DMEM (negative control), DMEM containing 5% FBS (reference), or DMEM containing 10% FBS (positive control). When the free drug was used, vancomycin or meropenem was solubilized directly in DMEM supplemented with 5% FBS, sterile-filtered, and 100 µL applied to hDFA cells. The free drug concentration range represents the maximum concentrations used within conventional bacterial broth microdilution susceptibility testing and those expected to be achieved upon 24-hour release of vancomycin or meropenem from loaded GSH-PEG hydrogels (~0.7 mg/mL [1.4±0.1 mg/24h] vancomycin and approximately 0.2 mg/mL [0.4±0.0 mg/24h] meropenem).[42] Cells were incubated for 24 hours in the specified conditions prior to being washed three times with 200 µL DPBS and quantified via Promega CellTiter96 Assay, per manufacturer instructions. Relative cell proliferation (CP), as a percentage (%) compared to the reference hDFA in DMEM 5% FBS, was calculated (Equation 1).

$$CP\ (\%) = \frac{Cells\ in\ test\ sample}{Cells\ in\ DMEM\ 5\%\ FBS} \text{ X } 100 \quad \text{Equation 1}$$

hDFA Migration

Cells were seeded at a density of 2,000 cells per chamber of an Ibidi cell culture insert housed within a 12-well plate and allowed to adhere. Following 24 hours, cell culture inserts were removed, cell patches were washed twice with 0.5 mL DPBS, and 0.5 mL DMEM supplemented with 0% or 5% FBS. Concurrently, sterilized hydrogels were loaded with or without the drug in DMEM (vancomycin [32 mg/mL] or meropenem [16 mg/mL]) for 1 hour prior to the brief DPBS wash. Prepared hydrogels were transferred to transwell inserts, placed into the respective cell culture well containing DMEM with 5% FBS, and allowed to co-incubate for 48 hours. For pre-incubation studies, unloaded hydrogels were placed into 0.5 mL of DMEM containing 5% FBS for 24 hours within a humidified 37°C incubator prior to being transferred for co-incubation with hDFA. Migration of hDFA was captured using an Olympus IX microscope under 10x and 40x magnification at 0, 24, and 48 hours. Captured images were analyzed using ImageJ v.1.52 with the aid of an image analysis script (File S1).[51] Relative area reduction (AR), as a percentage (%) of the control, at each time (t), as compared to the initial cell-free area for each individual sample, was calculated (Equation 2).

$$AR_t\ (\%) = \frac{Cell\ free\ area\ at\ time\ t}{Cell\ free\ area\ at\ time\ 0} \text{ X } 100 \quad \text{Equation 2}$$

Susceptibility Testing of Mature Biofilms

Following the assessment of biofilm formation detailed in the S.I., bacterial isolates including *P. aeruginosa* strains ATCC27853, AR0514, **and** AR0440, and *S. aureus* strains AR0479, AR0565, AR0219 were selected for further biofilm evaluation as the strongest biofilm-forming strains for each species. Biofilms were initially established by adding an inoculum of approximately 5 x 10^8 CFU/well to a 48-well plate, followed by incubation at 37°C for 24 hours. Post incubation, the wells were gently washed once with DPBS. Subsequently, 500 µL of CAMHB, either without antibiotics or containing varying concentrations of vancomycin (100 to 2,000 µg/mL for *S. aureus*)[52] or meropenem (0.5 to 1,000 µg/mL for *P. aeruginosa*),[53] was added to the respective wells. After a further 24-hour incubation, the biofilm biomass was quantified using the crystal violet staining method[54] as described in the S.I.

Eradication of Mature Biofilms

For the evaluation of biofilm disruption, bacterial suspensions (4 x 10^8 CFU/well) were seeded into 48-well plates and incubated at 37°C for 24 hours to promote biofilm formation. After washing with DPBS, treatment groups were established as follows: (1) DPBS only (negative control); (2) unloaded GSH-PEG hydrogel; (3) vancomycin-loaded GSH-PEG hydrogel for *S. aureus* biofilms or meropenem-loaded GSH-PEG hydrogel for *P. aeruginosa* biofilms; and (4) the corresponding free vancomycin or meropenem solution. Treatments were prepared in a total volume of 500 µL per well, consisting of 400 µL of medium and 100 µL of DPBS or antibiotic solution. After 24 hours of further incubation, the biofilm biomass was measured using the crystal violet staining technique,[54] as detailed in the S.I.

Biofilm Adhesion

Following the assessment of biofilm eradication, the hydrogels from each experimental group were carefully retrieved and immersed in 1 mL of DPBS for sonication. To dislodge biofilm cells that remained attached to the hydrogels, each sample underwent 3 cycles of sonication in a water bath sonicator with 45 seconds on and 15 seconds off. Then, the supernatant was serially diluted in DPBS using logarithmic intervals. Aliquots of 50 µL were plated onto agar plates using either an L-shaped cell spreader or a WASP Touch spiral plating system (Don Whitley Scientific). These plates were then incubated at 37°C for 24 h, followed by colony counting using the ProtoCOL3 Plus automated colony counter (Synbiosis).[55, 56] A greater than or equal to (≥) 3 log reduction in CFU/mL (99.9% kill) relative to the

View Article Online
DOI: 10.1039/D5TB02910H

initial inoculum was considered indicative of bactericidal activity.[57]

Protein Adhesion

Protein adhesion was assessed using bovine serum albumin, as a model protein. Hydrogels were equilibrated in 5 mL of DPBS for 3 days with 2 buffer changes per day and equilibrated at 37°C overnight prior to use in experiments. Cotton gauze, prepared as single-ply and cut to match the hydrogel surface area (~1.4 cm^2), was equilibrated identically. Fatty acid-free bovine serum albumin was dissolved to a final concentration of 30 mg/mL in DPBS and warmed to 37°C for 15 minutes. Equilibrated materials were placed into Falcon 48-well cell culture plates and 0.5 mL of protein solution was added to each well. Materials were incubated in the protein solution at 37°C for 24 hours. After 24 hours, the solution was removed, and materials were transferred to a 2-mL microcentrifuge tube. To remove adsorbed protein, 0.5 mL of 5% sodium dodecyl sulfate (SDS) solution was added to each sample and boiled for 10 minutes. The solution was transferred to new microcentrifuge tubes. Bicinchoninic acid (BCA) protein quantification assay was used according to the manufacturer's directions to determine protein concentration per surface area.

Bacterial Adhesion

PEG, GSH-PEG, and gauze were prepared as outlined in the protein adhesion assay section above and UV-sterilized prior to use. Bacterial isolates (ATCC27853, ATCC29213, and ATCC33591) were prepared as suspensions in DPBS and diluted to a final starting concentration of 1 x 10^6 CFU/mL per well. PEG, GSH-PEG, and gauze were placed into 24-well plates containing 2 mL of bacterial suspension in CAMHB per well and incubated at 35°C with shaking to ensure log-phase growth. A 20 µL aliquot was obtained at 0 and 24 h from each well for quantification of bacterial growth in the CAMHB in the presence of materials. After 24 hours, materials were washed twice in 5 mL of DPBS prior to being transferred to 1 mL of DPBS for sonication. Sonication and subsequent procedures for quantifying viable bacteria were performed as described in the Biofilm Adhesion subsection.[55, 56]

Statistical Analyses

Data are presented as the mean ± standard deviation of triplicate experiments. Brown-Forsynthe and Welch ANOVA with Dunnett's T3 multiple comparisons test was utilized for comparisons between groups due to the assumption of unequal standard deviation. A *p*-value of ≤0.05 was considered statistically significant. GraphPad Prism was utilized for all statistical analysis.

Results & Discussion

Bacterial Growth Inhibition Following Antibiotic Delivery

GSH-PEG hydrogels demonstrated activity against Gram-positive and Gram-negative isolates through selective antibiotic delivery; no growth inhibition was observed using blank hydrogels against all isolates (**Figure 1**). Following the release of vancomycin from GSH-PEG hydrogels into agar media, zones of growth inhibition (ZOIs) were observed against Gram-positive *S. aureus* isolates (**Figure 1A**). Following the release of meropenem from GSH-PEG hydrogels into solid agar, growth inhibition of Gram-negative *P. aeruginosa* isolates was achieved for all isolates except for CNP23 (**Figure 1B**). Due to the lack of activity of meropenem, the susceptibility profile of the CNP23 isolate was used to select amikacin for directed, susceptibility-based delivery (**Figure 1C**). As expected, the resulting ZOI from the amikacin delivered via GSH-PEG was identical for CNP23 and another amikacin-susceptible isolate with equivalent MIC (*p* = 0.6433).

Treatment failure in ABSSSIs has been attributed to poor tissue vancomycin penetration.[13] Unfortunately, dose-limiting toxicities of vancomycin prevent clinicians from simply increasing systemic doses to achieve adequate target site concentrations.[15, 16] Vancomycin-loaded GSH-PEG hydrogels offer a promising option for overcoming the drug-level treatment barriers for *S. aureus* infections through controlled, local delivery. Vancomycin released from GHS-PEG hydrogels inhibited the growth of methicillin-susceptible and methicillin-resistant *S. aureus* (MSSA [ATCC29213] and MRSA [ATCC33591], respectively) in addition to VISA strains (**Figure 1A**). It is important to note our studies were not intended to discern isolate susceptibility based on ZOI, as may be completed with disk diffusion assays according to CLSI standards.[48, 58, 59] Nevertheless, these experiments indicate the drug can be released from the hydrogel, diffuse through agar, and maintain antibacterial activity.

View Article Online
DOI: 10.1039/D5TB02919H

ARTICLE

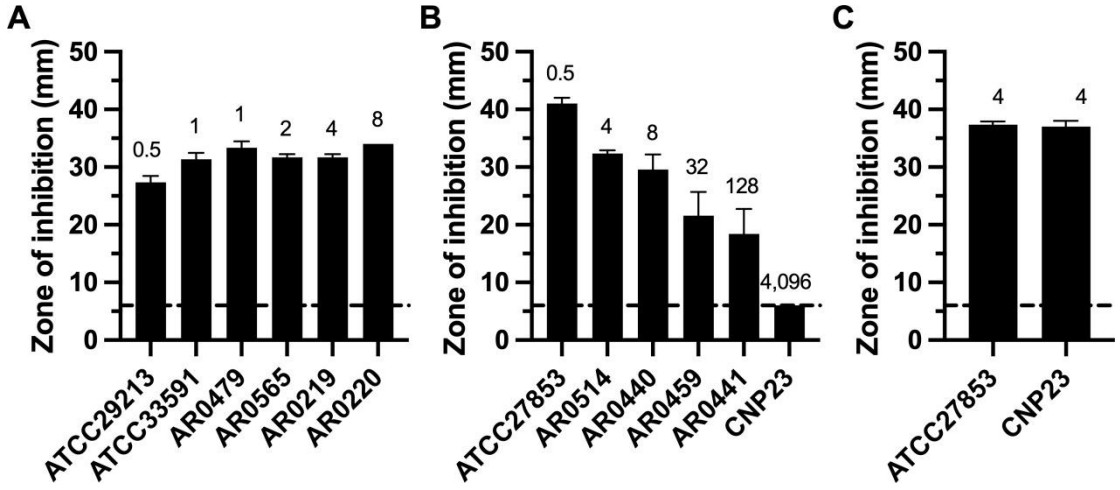

Figure 1. Bacterial growth inhibition was achieved by antibiotic-loaded GSH-PEG hydrogels. Release of (A) vancomycin against varying *S. aureus* isolates, (B) meropenem against *P. aeruginosa* isolates, and (C) amikacin against *P. aeruginosa* isolates. The dashed lines (- -) are equivalent to the hydrogel diameter, demonstrating a lack of bacterial growth inhibition from blank hydrogels. Columns and bars represent the mean plus or minus (±) the standard deviation of three independent experiments. The numbers above the bars denote the isolate's MIC (μg/mL).

Gram-negative bacteria, however, are a growing concern in ABSSSIs and are not susceptible to vancomycin. Gram-negative bacteria in ABSSSIs are often overlooked and inappropriately addressed through empiric therapy, increasing the risk of worsening infection and/or development of necrotizing fasciitis.[2] Our initial report on GSH-PEG hydrogels demonstrated varying growth inhibition against two *P. aeruginosa* isolates, one meropenem-susceptible and one resistant as a result of meropenem delivery.[42] Expanding upon initial findings, meropenem-loaded GSH-PEG hydrogels inhibited the growth of intermediate (MIC 4 μg/mL) and some resistant (MIC ≥ 8 μg/mL) *P. aeruginosa* isolates (**Figure 1B**). Despite traditionally being among the most active agents against Gram-negative bacteria, the effectiveness of carbapenems is being challenged by the increasing prevalence of bacterial resistance mechanisms, such as carbapenemase enzymes and mutations to outer membrane porin channels.[60-62] While simply increasing carbapenem concentrations systemically is limited by patient safety concerns, alternative strategies to overcome such resistance mechanisms are an area of active research.[56, 62, 63] Notably, localized delivery of meropenem via GSH-PEG was capable of achieving growth inhibition in one of the two carbapenemase-containing isolates [AR0441 but not CNP23]. Further investigation is warranted to examine the activity of localized, concentrated meropenem delivery for bacterial isolates with different carbapenemase enzymes, expression levels, and MICs. One key benefit of the GSH-PEG hydrogels is that the GSH-PEG hydrogels can provide a flexible delivery platform to target and exploit isolate susceptibilities. As a proof of concept, the GSH-PEG hydrogel was loaded with amikacin to target CNP23, which was not inhibited by meropenem but is susceptible to amikacin. The release of amikacin led to growth inhibition of the CNP23 isolate (**Figure 1C**), supporting the potential of susceptibility-guided therapy with GSH-PEG hydrogels.

These findings suggest that GSH-PEG hydrogels can be selectively loaded and release antibiotics to overcome Gram-positive and Gram-negative organisms, including isolates that are traditionally defined as resistant. Electrostatic and hydrogen bonding intermolecular forces have been demonstrated to influence the association and release of antibiotics from the GSH-PEG hydrogels.[42] The dissociation of antibiotics from GSH ligands and their subsequent diffusion into agar resulted in bacterial growth inhibition. However, localized antibiotic delivery poses a potential risk of local toxicity to dermal tissues.

Influence of GSH-PEG on Fibroblast Proliferation and Migration

Having examined localized antimicrobial delivery against several antibiotic-resistant bacterial isolates, dermal fibroblast responses to GSH-PEG hydrogels as an initial measure of host cell compatibility relevant to wound-facing applications was evaluated. The proliferation and migration of hDFA cells are critical in the remodeling and closure of skin wounds.[35, 36] Two separate, complementary assays with these cells were employed that investigated the influence of GSH-PEG with and without antibiotics on proliferation and migration.[50, 64, 65] First, the temporal response of hDFA cells to co-incubation with the GSH-PEG hydrogels was evaluated, quantifying hDFA migration across a cell-free gap (**Figure 2A**).[50, 66] Following 24 hours of

exposure, hDFA recovered an area greater than 50% in all tested groups with the exception of serum-starved hDFA control (**Figure 2B**). Hydrogel-naïve hDFA demonstrated an 83.4±13.9% recovery after 24 hours, whereas the groups with hydrogels present resulted in 60.6±8.1%, 58.5±2.0%, and 55.6±12.4% recovery for blank, vancomycin-loaded, and meropenem-loaded GSH-PEG, respectively. Following 48 hours of co-incubation, hDFA migration in the presence of blank, vancomycin-loaded, and meropenem-loaded GSH-PEG was indiscernible from hydrogel-naïve hDFA (96.2±2.2%, 98.1±1.1%, and 94.6±0.5% vs. 98.9±1.1% area reduction, respectively), whereas serum-starved area recovery remained below 50% (34.9±19.2%; **Figure 2C**). As such, there may be an initial growth inhibition due to the presence of the hydrogel that is recovered over time. This initial inhibition could be related to nutrient transfer, components from the hydrogels, or the loaded bioactive molecules.

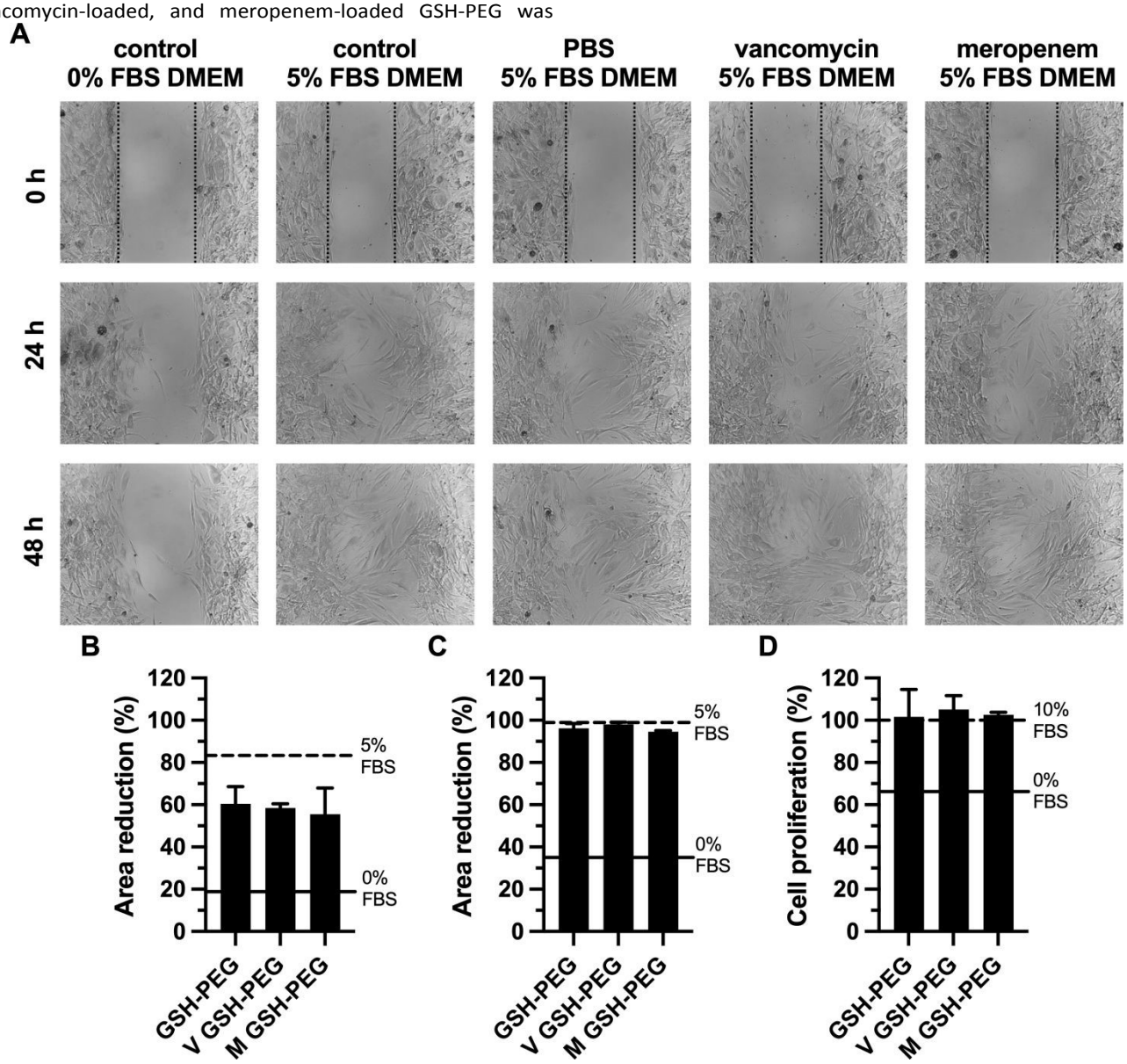

Figure 2. hDFA migration and proliferation in the presence of hydrogels. Representative images of hDFA migration (A) with black lines demarking initial cell gap area at 0 hours. Recovery of the cell-free gap area at 24 hours (B) and 48 hours (C) by hDFA in the presence of blank, vancomycin (V), or meropenem (M)-loaded GSH-PEG hydrogels or hydrogel-naïve conditions in serum-starved media (|; 0% FBS) or serum-supplemented media (--; 5% FBS). Proliferation of hDFA following 24-hour treatment with conditioned media obtained from blank, V, or M-loaded GSH-PEG (D). Cell proliferation is expressed as a % comparison to hDFA proliferation in hydrogel-naïve, serum-supplemented (- -; 5% FBS); serum-starved (—; 0% FBS) and serum-rich (···; 10% FBS) conditions serve as controls. Columns and bars represent the mean plus or minus (±) the standard deviation of three independent experiments.

In the second approach, hDFA proliferation was examined in the presence of peak drug concentrations obtained from hydrogel release. As compared to the preceding approach examining the effect of temporal drug release, the present method used conditioned media to gauge the impact of peak drug concentration released from the hydrogels. Following 24-hour incubation, hDFA proliferation in conditioned media obtained from blank, vancomycin-loaded, or meropenem-loaded GSH-

View Article Online
DOI: 10.1039/D5TB02010H

PEG was 98.1±3.7%, 101.8±4.0%, and 101.0±4.1% of that in unconditioned media (5% FBS; **Figure 2D**). Furthermore, GSH-PEG did not enhance or retard hDFA proliferation, as observed in drug-naïve serum-supplemented (10% FBS) or serum-starved conditions (0% FBS), respectively. Tolerance of hDFA to simulated peak drug concentrations was confirmed upon exposing cells to free drug at the upper limit concentrations found within traditional MIC testing (1,024 μg/mL); minimal influence on proliferation was encountered (**Figure S1**).

In accordance with the response to free drug concentrations (**Figure S1**), neither blank nor loaded GSH-PEG hydrogels were observed to significantly alter hDFA proliferation and migration as compared to hydrogel-naïve conditions (p>0.05 for all). Although hDFA migration was diminished in the presence of GSH-PEG during the initial 24 hours of hydrogel co-incubation (**Figure 2B**), no significant difference in migration was observed after 48 hours (**Figure 2C**). The observed lag in hDFA migration may be attributed to serum protein adsorption to hydrogel surface during the initial phase of incubation, resulting in diminished protein supplementation as compared to hydrogel-naïve hDFA at 24 hours. In support of this hypothesis, no lag phase was observed when the GSH-PEG hydrogels were pre-incubated for 24 hours in FBS-containing media prior to hDFA exposure (**Figure S2**).

Collectively, these results support hDFA are not negatively impacted by treatment with the hydrogels; proliferation was not impacted and migration minimally impacted following exposure to blank and antibiotic-loaded GSH-PEG hydrogels under the tested conditions. Future studies using complementary co-culture wound models and expanded biological endpoints will further define the translational compatibility of the approach.

Reduction of Biofilm Growth with GSH-PEG-mediated Antibiotic Delivery

Wound infections can delay healing and may persist through the formation of microbial biofilms, which are clustered communities of microorganisms embedded in a self-produced matrix of extracellular polymeric substances (EPS), including polysaccharides, proteins, and lipids.[67, 68] This matrix is interspersed with a network of channels for the flow of water and nutrients.[69] Biofilms may exhibit over a 1,000-fold increase in resistance to systemic antibiotics compared to free-floating, planktonic bacteria[70] necessitating the administration of broad-spectrum antibiotics at concentrations significantly above typical therapeutic dosages[71]. This may increase the risk of adverse effects and further worsen the antibiotic-resistance crisis.[67, 72] Alternative approaches are needed to achieve locally high concentrations of therapeutics needed to maximize killing of biofilm-embedded bacteria. In this context, assessing mature biofilm responses extends prior antibacterial evaluation by addressing a more treatment-relevant barrier to wound infection resolution.

Polymeric hydrogels have gained growing attention as therapeutic platforms for combating biofilm-associated infections. Their hydrated, porous nature mimics the natural extracellular matrix, enabling high water content, oxygen permeability, and tissue compatibility. Importantly, hydrogels can act as localized reservoirs for antibacterial agents, facilitating their sustained release within the wound environment—an essential feature given the diffusion-limiting barrier posed by the EPS in mature biofilms. This delivery potential, combined with their tunable physicochemical characteristics (e.g., redox responsiveness, surface charge, or degradation kinetics), positions hydrogels as a versatile class of materials not only for preventing bacterial colonization but also for penetrating and disrupting established biofilm structures.[73]

Recognizing the potential of antibiotic-loaded GSH-PEG hydrogels for biofilm eradication, we initiated our investigation by assessing the biofilm formation potential of six different strains of *P. aeruginosa* and *S. aureus*. Among the *P. aeruginosa* isolates, five demonstrated strong biofilm production (optical density (OD) > 4 × optical density cut-off value (ODc)), with the exception of AR0054, which was classified as a weak biofilm producer (ODc < OD ≤ 2 × ODc) (**Figure S3**). Conversely, the biofilm formation ability of the *S. aureus* isolates was generally lower; four of the six strains were identified as weak biofilm producers (ODc < OD ≤ 2 × ODc; strains ATCC29213, AR0479, AR0565, AR0219). The remaining two strains, ATCC33591 and AR0220, did not produce biofilms (OD ≤ ODc)(**Figure S3**). Based on these results, three *P. aeruginosa* strains (ATCC27853, AR0514, AR0440), identified as strong biofilm producers, and three *S. aureus* strains (AR0479, AR0565, AR0219), noted for their relatively higher biofilm formation potential among the weak producers, were selected.

In evaluating the susceptibility of mature biofilms to antibiotics, vancomycin significantly reduced viable bacteria in mature *S. aureus* biofilms at all tested doses (p < 0.0001) compared to untreated controls. However, increasing the concentration beyond 100 μg/mL did not further enhance antibiofilm efficacy (**Figure 3A**). This concentration-independent behavior is consistent with previous findings in mature biofilm models, where vancomycin activity showed limited improvement at higher doses.[52] Similar plateau effects have also been reported with other antibiotics, such as tobramycin and polymyxin B, in *P. aeruginosa* biofilms.[71] Such a profile highlights the importance of optimizing delivery strategies to maintain effective local concentrations without relying on high dosing. For meropenem, antibiofilm responses varied across *P. aeruginosa* strains and appeared influenced by both isolate-specific susceptibility and dose (**Figure 3B**). In the susceptible ATCC 27853 strain, biofilm biomass was significantly reduced at 5 μg/mL, with no additional benefit at higher concentrations. In contrast, AR0440 showed no significant reduction in biomass at concentrations up to 5 μg/mL, with a consistent decrease observed only at concentrations greater than or equal to 100 μg/mL. Although the slight increase at sub-inhibitory doses was not statistically significant, this pattern aligns with prior reports suggesting that low-dose β-lactam antibiotics can stimulate biofilm formation, likely through stress-induced gene regulation and enhanced matrix production.[74] AR0514 isolate showed no significant biomass reduction at any dose, indicating robust biofilm-associated tolerance. Together, these findings emphasize the need for tailored local delivery strategies that account for strain-specific and non-linear antibiotic responses.

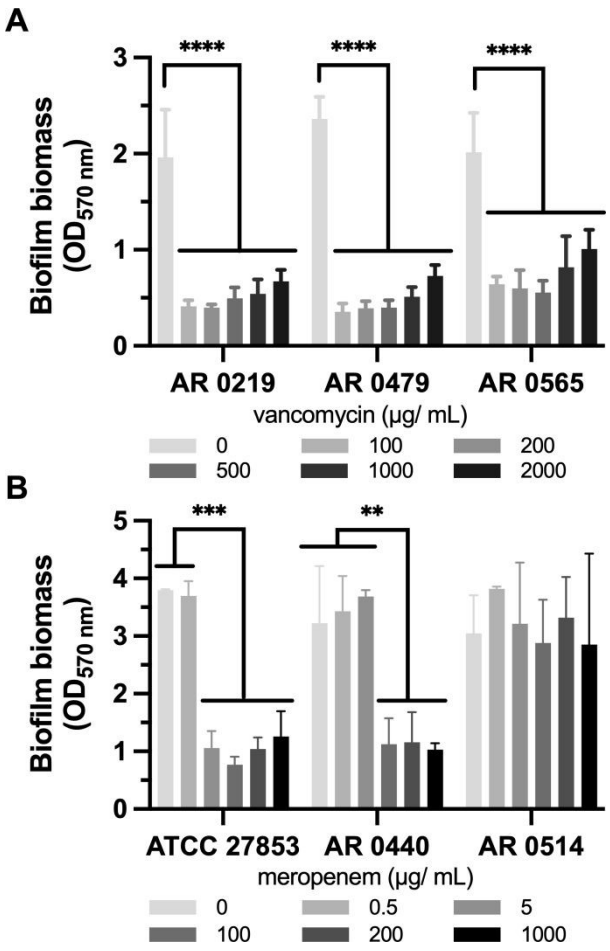

Figure 3. Biofilm biomass is reduced by treatment with antibiotic. Quantification of biofilm biomass by crystal violet staining following 24-hour exposure of *S. aureus* (A) and *P. aeruginosa* (B) biofilms to vancomycin and meropenem, respectively. Columns and bars represent the mean plus or minus (±) the standard deviation of three independent experiments. **p<0.01, ***p<0.001, ****p<0.0001.

Building on the susceptibility results, we next evaluated the antibiofilm activity of vancomycin-loaded GSH-PEG hydrogels in the same three *S. aureus* strains following 24-hour treatment, including a free vancomycin group at a concentration equal to the hydrogel's released amount (**Figure 4A**). GSH-PEG–vancomycin significantly reduced biomass compared to untreated controls, with reductions of 61.4 ± 10.3% (AR0219), 63.1 ± 13.6% (AR0479), and 75.4 ± 7.2% (AR0565). Against AR0219, the loaded hydrogel also outperformed free vancomycin ($p < 0.05$), suggesting that localized hydrogel-based delivery enhances antimicrobial performance, likely through sustained local concentrations, improved retention within the biofilm matrix, and potential contributions from the hydrogel's intrinsic activity. While similar trends were observed in AR0479 and AR0565, the differences relative to free vancomycin were not statistically significant.

Interestingly, the unloaded GSH-PEG hydrogel also reduced biofilm biomass in all strains, with a statistically significant effect found in AR0565 ($p < 0.001$), indicating inherent antibiofilm activity of the polymer itself. This response may reflect the combined influence of the hydrated PEG network and accessible pendant amine and carboxyl groups from GSH at the hydrogel–biofilm interface. Prior studies have shown that zwitterionic materials can resist biofouling through the formation of highly hydrated interfacial layers that reduce nonspecific adhesion.[75]

The strain-specific nature of this effect—most pronounced in AR0565—may be attributed to differences in EPS composition, charge density, or matrix structural organization, which may alter biofilm interactions with the hydrogel surface. Collectively, these findings suggest that GSH-PEG hydrogels not only enhance vancomycin efficacy through sustained and localized delivery but may also influence biofilm stability in a species- and strain-dependent manner.

Extending this investigation to *P. aeruginosa*, GSH-PEG–meropenem significantly reduced biofilm biomass across all tested strains—ATCC 27853, AR0440, and AR0514—with reductions of 82.5 ± 2.1%, 82.5 ± 9.7%, and 60.9 ± 16.5%, respectively, relative to untreated controls (**Figure 4B**). Although mean biomass values were lower than those observed with free meropenem in ATCC 27853 and AR0440, the differences did not reach statistical significance.

Notably, unloaded GSH-PEG hydrogels failed to produce a significant antibiofilm effect in any of the *P. aeruginosa* strains, contrasting with the response noted in *S. aureus* AR0565. This absence of activity points to the species-specific difference in how biofilms interact with the hydrogel surface, possibly because of more robust matrix architecture or reduced sensitivity to physicochemical perturbations. Collectively, these findings underscore the potential of GSH-PEG hydrogels to enhance antibiotic efficacy across both Gram-positive and Gram-negative pathogens, while highlighting that any non-drug-mediated effects on biofilm integrity are likely context-dependent—shaped by the interplay of bacterial species, strain-level traits, and surface chemistry.

Biologic materials within wound exudate are known to adsorb onto dressing materials through hydrophobic, electrostatic, and hydrogen bonding interactions, which in turn may initially slow wound healing processes.[27, 28, 32, 43, 76] The GSH-PEG hydrogels exhibit similar potential to impede initial wound healing processes due to sorption of protein upon hydrogel introduction to cell media. However, the presence of a bacterial infection precludes any host efforts from achieving timely wound closure.[34, 36, 77] The GSH-PEG hydrogels are intended to deliver antimicrobials for ABSSSI clearance and thus facilitate wound resolution. If clinician's concern shifts towards potential material biofouling following ABSSSI clearance, the clinician would maintain the option to replace the GSH-PEG hydrogel with an alternative dressing material. To compare protein association across gauze, PEG, and GSH-PEG surfaces, adsorption was quantified by albumin as a model protein.

View Article Online
DOI: 10.1039/D5TB02310H

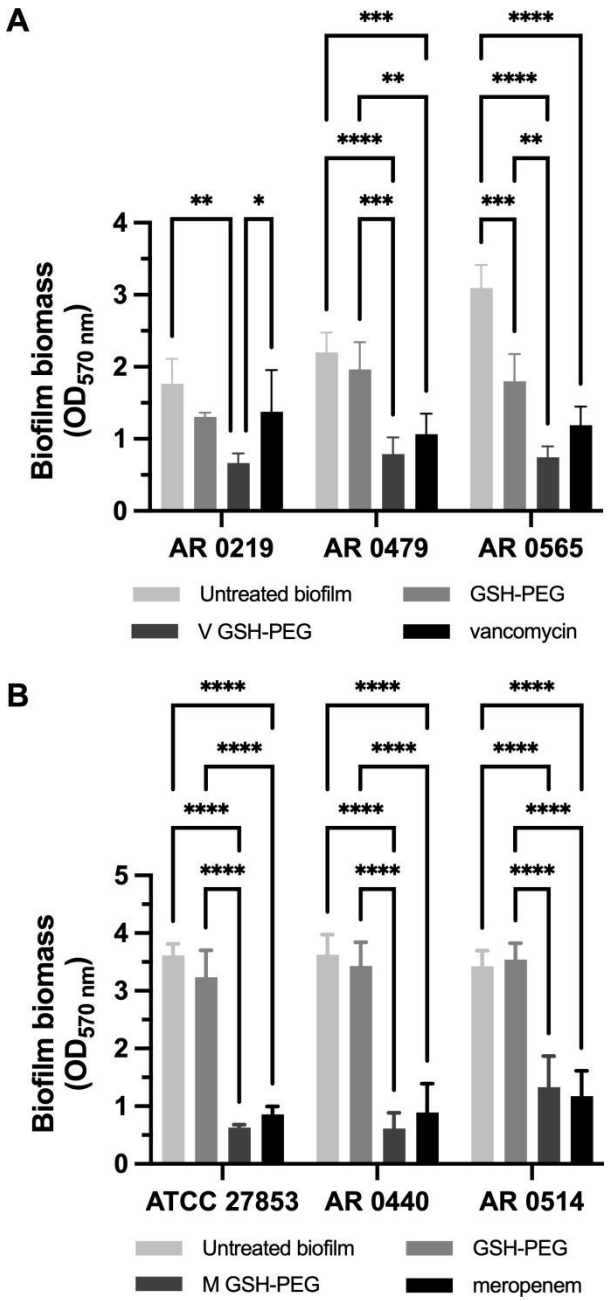

Figure 4. **Biofilm biomass is reduced following treatment with GSH-PEG antibiotic loaded hydrogels.** Biofilm biomass was quantified by crystal violet staining after 24 h treatment of *S. aureus* (A) and *P. aeruginosa* (B) biofilms with DPBS only, unloaded GSH-PEG hydrogel, vancomycin- or meropenem-loaded GSH-PEG hydrogel (V GSH-PEG and M GSH-PEG, respectively), or the corresponding free antibiotic. Values represent the mean plus or minus (±) the standard deviation of three independent experiments. *p<0.05, **p<0.01, ***p<0.001, ****p<0.0001.

Biofouling to material surfaces

Protein fouling onto biomaterials is believed to occur upon the formation of favorable hydrogen bonds or electrostatic interactions between proteins and materials.[44, 45] Materials such as cotton may also physically trap proteins and allow for hydrophobic interactions.[78] Reduction in surface protein association may be achieved by favoring interaction with water at the biomaterial surface to create a solvation shell, through use of zwitterionic moieties or ether groups, such as those within PEG.[45] However, despite PEG-based materials often being considered the preferred material to achieve "anti-fouling", adsorption of biological materials is not completely eliminated.[79-81]

As compared to conventional cotton gauze dressings, a 79.3% and 95.1% reduction in surface serum albumin fouling was observed for PEG (p= 0.0020) and GSH-PEG (p= 0.0010) hydrogels, respectively (**Figure 5**). As compared to PEG-only, GSH-PEG hydrogels experienced 76% less albumin fouling (p= 0.0001). The use of albumin as a model protein enabled comparison of adsorption behavior across material surfaces and showed reduced protein fouling for GSH-PEG hydrogels under the tested conditions. Our findings are consistent with previous reports describing lower protein fouling on polymeric surfaces upon incorporation of zwitterionic functionalities.[43, 45, 82, 83]

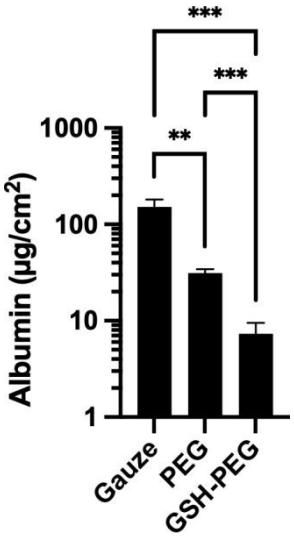

Figure 5. **Fouling of albumin to material surfaces.** Following 24-hour incubation, cotton gauze, PEG, or GSH-PEG hydrogels were boiled to disrupt adsorbed protein. Values represent the mean plus or minus (±) the standard deviation of at least four independent experiments. **p<0.001, ***p<0.001. Brown-Forsynthe and Welch-corrected ANOVA test with Dunnett's T3 multiple comparison test for pairwise comparison.

Bacterial adhesion to dressing materials is an equally pressing concern within ABSSSI treatment and wound healing, posing the risk of biofilm formation.[21, 34, 77, 82, 84, 85] Following 24-hour incubation with *P. aeruginosa* (**Figure 6A**), GSH-PEG hydrogels reduced bacterial adsorption as compared to conventional cotton gauze materials (-2.6±0.3 log, p=0.0014) whereas PEG hydrogels yielded similar adsorption as cotton gauze (-1.2±0.4 log, p=0.1482). Both GSH-PEG and PEG hydrogels showed reduced surface adsorption of methicillin-sensitive *S. aureus* (MSSA; **Figure 6B**) compared to cotton gauze; however, these reductions were not statistically significant (-1.3 ± 0.4 log, p = 0.1200 for GSH-PEG; -1.2 ± 0.3 log, p = 0.0689 for PEG). Surface adsorption of methicillin-resistant *S. aureus* (MRSA; **Figure 6C**) was reduced with GSH-PEG (-1.6±0.2 log, p=0.0084) and PEG (-1.2±0.2 log, p=0.0137) hydrogels as compared to cotton gauze. Overall bacterial growth was not influenced by the tested materials (**Figure S4**).

View Article Online
DOI: 10.1039/D5TB02919H

ARTICLE

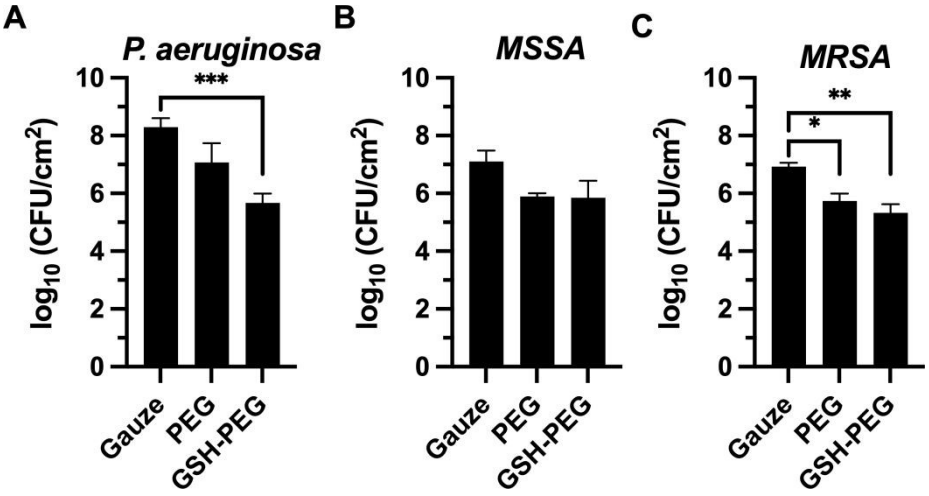

Figure 6. Log transformed bacterial colony forming units (CFU) adsorbed per material surface area. Cotton gauze, PEG, or GSH-PEG hydrogels, in the absence of any antibiotic, were incubated for 24 hours in the presence of *P. aeruginosa* (ATCC 27853, A), methicillin-sensitive *S. aureus* (ATCC 29213, B), or methicillin-resistant *S. aureus* (ATTC 33591, C) prior to sonication and agar plating. Columns and bars represent the mean plus or minus (±) the standard deviation of three independent experiments. * p<0.05, **p<0.01, ***p<0.001. Brown-Forsynthe and Welch-corrected ANOVA test with Dunnett's T3 multiple comparison test for pairwise comparison.

As compared to PEG hydrogels, bacterial adsorption to GSH-PEG surfaces was similar for *P. aeruginosa* (**Figure 6A**; -1.4±0.5 log, *p*=0.1101), MSSA (**Figure 6B**; 0.0±0.5 log, *p*=0.9985), and MRSA (**Figure 6C**; -0.4±0.2 log, *p*=0.3382) isolates. These findings indicate that GSH-PEG hydrogels reduced bacterial adhesion under the tested conditions, particularly relative to cotton gauze, while differences relative to PEG alone were modest and varied by bacterial species and strain. Differing bacterial responses to surfaces are not unexpected as inter- and intra-species differences in bacterial surface adherence and subsequent biofilm formation are known to exist.[86-88] Nonetheless, our findings support previous reports of reduced surface biofouling with the use of PEG-based and zwitterionic polymeric coatings.[81, 84-87]

We next examined the effects of antibiotic-loaded hydrogels on bacterial growth in liquid, expecting antibiotic release to reduce bacterial counts in culture and prevent adsorption. Co-incubation of *P. aeruginosa* and *S. aureus* isolates with loaded hydrogels containing meropenem or vancomycin, respectively, reduced bacterial bioburden in culture at 24 hours, achieving bactericidal activity for all isolates (**Figure 7A-C**). Furthermore, sonication of antibiotic-loaded hydrogels yielded no observable bacterial surface fouling following 24 hours of co-incubation (data not shown).

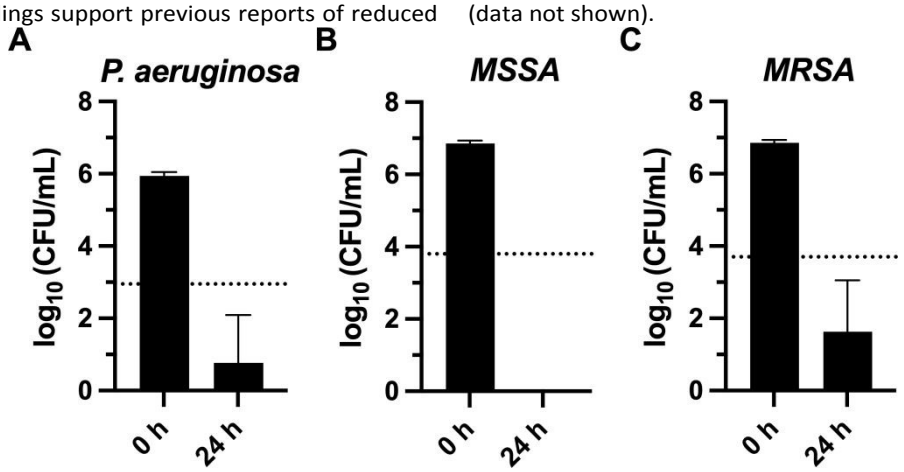

Figure 7. Bacterial growth and adherence following incubation with loaded GSH-PEG hydrogels. GSH-PEG hydrogels were loaded with meropenem against *P. aeruginosa* (ATCC 27853, A) and with vancomycin against methicillin-sensitive *S. aureus* (ATCC 29213, B) or methicillin-resistant *S. aureus* (ATTC 33591, C) prior to 24-

J. Mater Chem B ARTICLE

hour co-incubation in culture. The dashed line (…) denotes bactericidal activity, defined as ≥3 log reduction in CFU/mL from the starting inoculum. Columns and bars represent the mean plus or minus (±) the standard deviation of three independent experiments.

View Article Online
DOI: 10.1039/D5TB02919H

We then assessed the impact of antibiotic loading on biofilm adhesion to hydrogel surfaces. Vancomycin-loaded GSH-PEG hydrogels also significantly reduced biofilm adhesion compared to drug-free hydrogels (*p*-values: < 0.01 for AR0219, < 0.0001 for AR0479, and < 0.001 for AR0565) (**Figure 8A**). Similarly, meropenem-loaded GSH-PEG hydrogels exhibited a substantial reduction in surface biofouling for biofilms of *P. aeruginosa* strains compared to drug-free hydrogels. The reduction was particularly striking for ATCC27853, resulting in no CFUs after plating and incubation, indicating a complete inhibition of bacterial growth. For the other two strains, the reduction was significant (*p*-values < 0.0001) reflecting a substantial decrease in biofilm adhesion compared to drug-free hydrogels (**Figure 8B**).

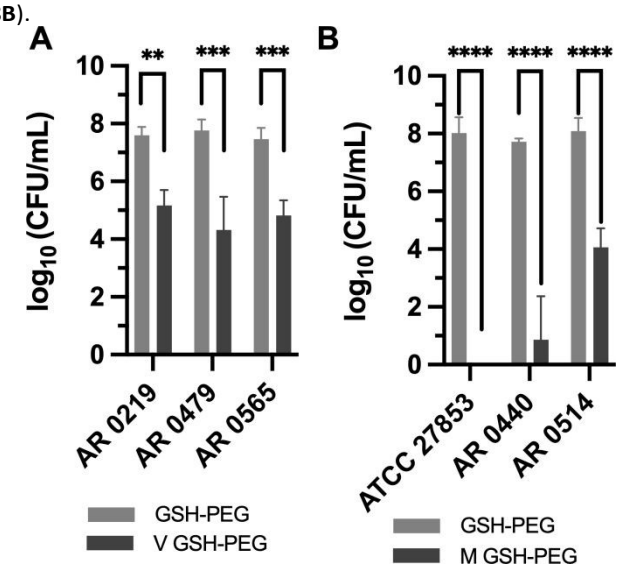

Figure 8. Viable *S. aureus* (A) or *P. aeruginosa* (B) bacteria adhered less to GSH-PEG hydrogels (GSH-PEG) when vancomycin (A; V GSH-PEG) or meropenem (B; M GSH-PEG) were present, following 24 hours of incubation with mature biofilms. Values represent the mean plus or minus (±) the standard deviation of three independent experiments. **p<0.01 ***p<0.001 ****p<0.0001.

Our present findings demonstrate decreased surface biofouling with polymeric hydrogels as compared to conventional gauze material. Protein adsorption, together with bacterial and biofilm adhesion studies, supported reduced surface fouling profile for GSH-PEG hydrogels under the tested conditions. Furthermore, the release of antibiotic agents successfully reduced bacterial bioburden in liquid culture and significantly decreased bacterial and biofilm adsorption to GSH-PEG hydrogels. Nonetheless, further investigation of inter- and intra-species variation is warranted, particularly in the absence of antibiotic loading. The reduced biofouling observed for GSH-PEG hydrogels represents a favourable interfacial property for wound dressing materials and suggests their potential to limit nonspecific adsorption and surface-associated contamination at the wound-material interface. In addition, antibiotic loading further reduced bacterial and biofilm burden at the hydrogel surface, supporting the ability of the platform to combine local antimicrobial delivery with favourable surface-associated performance under the tested conditions. Taken together, these findings extend prior validation of GSH-PEG hydrogels as local antibiotic delivery materials through further characterization of properties relevant to host response and interfacial behaviour that may influence performance at infected wound surfaces.

Conclusion

Hydrogels composed of GSH-conjugated to PEG polymers are attractive candidates for ABSSSI treatment. Initially intended for anchoring recombinant GST proteins, the zwitterionic tripeptide ligands have recently exhibited the ability to passively load small molecules through electrostatic and hydrogen bond interactions.[42] Herein, GSH-PEG hydrogels enabled localized delivery of selected antibiotics against a panel of Gram-positive and Gram-negative bacteria, while hDFA proliferation and migration studies suggested favorable initial host cell compatibility under the tested conditions. Furthermore, reduced protein, bacterial, and biofilm fouling under the tested conditions broadened the interfacial and biological characterization of the platform beyond antibiotic delivery alone. Collectively, these findings support further investigation of GSH-PEG hydrogels as a flexible and customizable platform for localized ABSSSI treatment.

Author Contributions

Karol Sokolowski: Methodology; Conceptualization; Investigation; Formal Analysis; Writing-Original Draft. **Sonia Alavi**: Methodology; Conceptualization; Investigation; Formal Analysis; Writing-Review& Editing. **Catherine F. Dial**: Methodology; Conceptualization; Investigation; Formal Analysis; Writing-Original Draft. **Zackery P. Bulman**: Methodology; Formal Analysis; Supervision; Writing-Review& Editing. **Richard A. Gemeinhart**: Methodology; Conceptualization; Formal Analysis; Supervision; Writing-Review& Editing; Funding Acquisition.

Conflicts of interest

Authors certify no potential conflicts of interest.

Acknowledgements

This work was supported in part by the W.C. and May Preble Deiss Fund for Biomedical Research and the Dean's Scholar Fellowship from the University of Illinois at Chicago (to K.S.). The authors thank Eric Wenzler for early feedback and input in the project and early review of the manuscript.

Artificial Intelligence (AI) Acknowledgement

Authors used AI in minor wordsmithing and English language improvements. Authors also used AI in doing some literature search; however, after AI support the literature was reviewed by the authors prior to citation.

References

1. S. A. Fritz, D. J. Shapiro and A. L. Hersh, Clin. Infect. Dis., 2020, 70, 2715-2718.
2. K. S. Kaye, L. A. Petty, A. F. Shorr and M. D. Zilberberg, Clin. Infect. Dis., 2019, 68, S193-S199.
3. E. Bouza and A. Burillo, Curr Opin Infect Dis, 2022, 35, 61-71.
4. A. Russo, E. M. Trecarichi and C. Torti, Curr Opin Infect Dis, 2022, 35, 95-102.
5. M. H. Wilcox and M. Dryden, J Antimicrob Chemother, 2021, 76, iv2-iv8.
6. K. Yadav, A. Nath, K. N. Suh, L. Sikora and D. Eagles, Infection, 2020, 48, 75-83.
7. K. S. Kaye, D. A. Patel, J. M. Stephens, A. Khachatryan, A. Patel and K. Johnson, PLoS One, 2015, 10, e0143276.
8. V. Vella, D. Derreumaux, E. Aris, M. Pellegrini, M. Contorni, M. Scherbakov and F. Bagnoli, Open Forum Infect Dis, 2024, 11, ofae267.
9. A. P. Grossi, A. Ruggieri, A. D. Vecchio, A. Comandini, L. Corio, F. Calisti, G. D. Loreto and B. Almirante, Int J Antimicrob Agents, 2022, 60, 106637.
10. A. Berger, G. Oster, J. Edelsberg, X. Huang and D. J. Weber, Surgical infections, 2013, 14, 304-312.
11. B. A. Lipsky, L. M. Napolitano, G. J. Moran, L. Vo, S. Nicholson and M. Kim, Diagnostic microbiology and infectious disease, 2014, 79, 273-279.
12. C. P. Montgomery, M. Z. David and R. S. Daum, Curr. Opin. Infect. Dis., 2015, 28, 253-258.
13. G. E. Stein and E. M. Wells, Current medical research and opinion, 2010, 26, 571-588.
14. B. Spellberg and L. B. Rice, Ann. Intern. Med., 2019, 171, 210-211.
15. M. N. Jeffres, Drugs, 2017, 77, 1143-1154.
16. S. C. J. Jorgensen, K. P. Murray, A. M. Lagnf, S. Melvin, S. Bhatia, M. D. Shamim, J. R. Smith, K. D. Brade, S. P. Simon, J. Nagel, K. S. Williams, J. K. Ortwine, M. P. Veve, J. Truong, D. B. Huang, S. L. Davis and M. J. Rybak, Infect. Dis. Ther., 2020, 9, 89-106.
17. V. Schechner, N. Fallach, T. Braun, E. Temkin and Y. Carmeli, J. Antimicrob. Chemother., 2021, 76, 2182-2185.
18. P. D. Tamma, E. Avdic, D. X. Li, K. Dzintars and S. E. Cosgrove, JAMA Intern. Med., 2017, 177, 1308-1315.
19. N. J. Onufrak, N. M. Smith, M. J. Satlin, J. B. Bulitta, X. Tan, P. N. Holden, R. L. Nation, J. Li, A. Forrest, B. T. Tsuji and Z. P. Bulman, Clin. Microbiol. Infect., 2020, 26, 1256.e1251-1256.e1258.
20. E. Wenzler, M. Santarossa, K. A. Meyer, A. T. Harrington, G. E. Reid, N. M. Clark, F. S. Albarillo and Z. P. Bulman, Open forum infectious diseases, 2020, 7, ofz545-ofz545.
21. S. Li, S. Dong, W. Xu, S. Tu, L. Yan, C. Zhao, J. Ding and X. Chen, Advanced science (Weinheim, Baden-Wurttemberg, Germany), 2018, 5, 1700527-1700527.
22. R. S. Kamath, D. Sudhakar, J. G. Gardner, V. Hemmige, H. Safar and D. M. Musher, Open forum infectious diseases, 2018, 5, ofx188.
23. J. W. Abetz, N. G. Adams and B. Mitra, Emerg Med J, 2018, 35, 56-61.
24. L. S. May, M. Zocchi, C. Zatorski, J. A. Jordan, R. E. Rothman, C. E. Ware, S. Eells and L. Miller, West. J. Emerg. Med., 2015, 16, 642-652.
25. D. L. Stevens, A. L. Bisno, H. F. Chambers, E. P. Dellinger, E. J. Goldstein, S. L. Gorbach, J. V. Hirschmann, S. L. Kaplan, J. G. Montoya, J. C. Wade and A. Infectious Diseases Society of, Clin. Infect. Dis., 2014, 59, e10-52.
26. D. A. Williamson, G. P. Carter and B. P. Howden, Clin. Microbiol. Rev., 2017, 30, 827-860.
27. J. S. Boateng, K. H. Matthews, H. N. E. Stevens and G. M. Eccleston, Journal of Pharmaceutical Sciences, 2008, 97, 2892-2923.
28. M. Madaghiele, C. Demitri, A. Sannino and L. Ambrosio, Burns & Trauma, 2014, 2, 153-161.
29. D. Simões, S. P. Miguel, M. P. Ribeiro, P. Coutinho, A. G. Mendonça and I. J. Correia, European Journal of Pharmaceutics and Biopharmaceutics, 2018, 127, 130-141.
30. K. Kalantari, E. Mostafavi, A. M. Afifi, Z. Izadiyan, H. Jahangirian, R. Rafiee-Moghaddam and T. J. Webster, Nanoscale, 2020, 12, 2268-2291.
31. G. Dabiri, E. Damstetter and T. Phillips, Advances in wound care, 2016, 5, 32-41.
32. A. Sood, M. S. Granick and N. L. Tomaselli, Advances in wound care, 2014, 3, 511-529.
33. K. LeBlanc, S. Baranoski, D. Christensen, D. Langemo, K. Edwards, S. Holloway, M. Gloeckner, A. Williams, K. Campbell, T. Alam and K. Y. Woo, Adv. Skin Wound Care, 2016, 29, 32-46.
34. O. Sarheed, A. Ahmed, D. Shouqair and J. Boateng, 2016.
35. I. Negut, V. Grumezescu and A. M. Grumezescu, Molecules (Basel, Switzerland), 2018, 23, 2392.
36. J. G. Powers, C. Higham, K. Broussard and T. J. Phillips, J Am Acad Dermatol, 2016, 74, 607-625; quiz 625-606.
37. S. L. Percival, P. G. Bowler and D. Russell, J Hosp Infect, 2005, 60, 1-7.
38. C. Gunawan, C. P. Marquis, R. Amal, G. A. Sotiriou, S. A. Rice and E. J. Harry, ACS Nano, 2017, 11, 3438-3445.
39. L. J. Wilkinson, R. J. White and J. K. Chipman, Journal of wound care, 2011, 20, 543-549.
40. J. S. Buhrman, J. E. Rayahin, M. Kollmer and R. A. Gemeinhart, BMC Biotechnol, 2012, 12, 63.
41. J. E. Rayahin, J. S. Buhrman and R. A. Gemeinhart, Eur J Pharm Sci, 2014, 65, 112-121.
42. K. Sokolowski, H. M. Pham, E. Wenzler and R. A. Gemeinhart, Pharm. Res., 2021, 38, 1247-1261.
43. K. T. Huang, Y. L. Fang, P. S. Hsieh, C. C. Li, N. T. Dai and C. J. Huang, Biomater Sci, 2017, 5, 1072-1081.
44. C. Blaszykowski, S. Sheikh and M. Thompson, Biomater Sci, 2015, 3, 1335-1370.
45. C. Leng, H. C. Hung, S. Sun, D. Wang, Y. Li, S. Jiang and Z. Chen, ACS Appl Mater Interfaces, 2015, 7, 16881-16888.
46. A. Andrianopoulou, K. Sokolowski, E. Wenzler, Z. P. Bulman and R. A. Gemeinhart, J Control Release, 2024, 365, 936-949.
47. J. S. Buhrman, L. C. Cook, J. E. Rayahin, M. J. Federle and R. A. Gemeinhart, J. Control. Release, 2013, 171, 288-295.
48. Clinical Laboratory Standards Institute, 2018.
49. Y. H. Xuan, B. B. Huang, H. S. Tian, L. S. Chi, Y. M. Duan, X. Wang, Z. X. Zhu, W. H. Cai, Y. T. Zhu, T. M. Wei, H. B. Ye, W. T. Cong and L. T. Jin, PLoS One, 2014, 9, e108182.
50. V. Moulin, G. Castilloux, A. Jean, D. R. Garrel, F. A. Auger and L. Germain, Burns, 1996, 22, 359-362.
51. C. A. Schneider, W. S. Rasband and K. W. Eliceiri, Nat. Methods, 2012, 9, 671-675.
52. V. Post, P. Wahl, R. G. Richards and T. F. Moriarty, Journal of orthopaedic research : official publication of the Orthopaedic Research Society, 2017, 35, 381-388.
53. M. J. Zahra, H. Hamed, R. Y. Mohammad, Z. Nosratollah, A. Akbarzadeh and M. Morteza, Artificial cells, nanomedicine, and biotechnology, 2017, 45, 975-980.
54. E. F. Haney, M. J. Trimble and R. E. W. Hancock, Nature protocols, 2021, 16, 2615-2632.
55. J. Borjan, K. A. Meyer, R. K. Shields and E. Wenzler, Int. J. Antimicrob. Agents, 2020, 55, 105852.
56. M. Biagi, T. Wu, M. Lee, S. Patel, D. Butler and E. Wenzler, Antimicrob. Agents Chemother., 2019, 63.
57. L. C. Nwabor, A. Chukamnerd, O. F. Nwabor, R. Pomwised, S. P. Voravuthikunchai and S. Chusri, Pharmaceuticals (Basel), 2023, 16.
58. A. O. Kshetry, N. D. Pant, R. Bhandari, S. Khatri, K. L. Shrestha, S. K. Upadhaya, A. Poudel, B. Lekhak and B. R. Raghubanshi, Antimicrob. Resist. Infect. Control, 2016, 5, 27.
59. S. Wongthong, K. Dutchanutouch, V. Namsaengkang, A. Chanawong, C. Wilailuckana and A. Lulitanond, J. Infect. Dev. Ctries., 2015, 9, 157-164.
60. B. Kitchel, D. R. Sundin and J. B. Patel, Antimicrob. Agents Chemother., 2009, 53, 4511-4513.
61. A. J. Brink, Curr. Opin. Infect. Dis., 2019, 32, 609-616.
62. F. S. Codjoe and E. S. Donkor, Medical sciences (Basel, Switzerland), 2017, 6, 1.
63. X. Tan, H. S. Kim, K. Baugh, Y. Huang, N. Kadiyala, M. Wences, N. Singh, E. Wenzler and Z. P. Bulman, Infection and drug resistance, 2021, 14, 125-142.
64. F. Ascione, A. Vasaturo, S. Caserta, V. D'Esposito, P. Formisano and S. Guido, Experimental Cell Research, 2016, 347, 123-132.
65. D. Chouhan, N. Dey, N. Bhardwaj and B. B. Mandal, Biomaterials, 2019, 216, 119267.
66. C. Tolg, P. Telmer and E. Turley, PLoS One, 2014, 9, e88479.
67. K. Kasza, P. Gurnani, K. R. Hardie, M. Cámara and C. Alexander, Advanced drug delivery reviews, 2021, 178, 113973.
68. X. Lv, L. Wang, A. Mei, Y. Xu, X. Ruan, W. Wang, J. Shao, D. Yang and X. Dong, Small (Weinheim an der Bergstrasse, Germany), 2023, 19, e2206220.
69. K. Sauer, P. Stoodley, D. M. Goeres, L. Hall-Stoodley, M. Burmølle, P. S. Stewart and T. Bjarnsholt, Nature reviews. Microbiology, 2022, 20, 608-620.
70. B. L. Price, R. Morley, F. L. Bowling, A. M. Lovering and C. B. Dobson, PLoS One, 2020, 15, e0228704.

View Article Online
DOI: 10.1039/D5TB02919H

71. X. Tan, Y. Huang, A. Rana, N. Singh, T. C. Abbey, H. Chen, P. T. Toth and Z. P. Bulman, NPJ Biofilms Microbiomes, 2024, 10, 16.
72. K. E. Grooters, J. C. Ku, D. M. Richter, M. J. Krinock, A. Minor, P. Li, A. Kim, R. Sawyer and Y. Li, Frontiers in cellular and infection microbiology, 2024, 14, 1352273.
73. A. Banerjee, P. Chowdhury, K. Bauri, B. Saha and P. De, Biomater Sci, 2022, 11, 11-36.
74. J. B. Kaplan, Int J Artif Organs, 2011, 34, 737-751.
75. P. Sae-ung, A. Wijitamornloet, Y. Iwasaki, P. Thanyasrisung and V. P. Hoven, Macromolecular Materials and Engineering, 2019, 304, 1900286.
76. V. Jones, J. E. Grey and K. G. Harding, BMJ (Clinical research ed.), 2006, 332, 777-780.
77. R. Edwards and K. G. Harding, Curr. Opin. Infect. Dis., 2004, 17, 91-96.
78. S. C. Goheen, J. V. Edwards, A. Rayburn, K. Gaither and N. Castro, in *Modified Fibers with Medical and Specialty Applications*, eds. J. V. Edwards, G. Buschle-Diller and S. C. Goheen, Springer Netherlands, Dordrecht, 2006, https://doi.org/10.1007/1-4020-3794-5_4, pp. 49-65.
79. T. Ekblad, G. Bergström, T. Ederth, S. L. Conlan, R. Mutton, A. S. Clare, S. Wang, Y. Liu, Q. Zhao, F. D'Souza, G. T. Donnelly, P. R. Willemsen, M. E. Pettitt, M. E. Callow, J. A. Callow and B. Liedberg, Biomacromolecules, 2008, 9, 2775-2783.
80. R. Michel, S. Pasche, M. Textor and D. G. Castner, Langmuir : the ACS journal of surfaces and colloids, 2005, 21, 12327-12332.
81. I. Banerjee, R. C. Pangule and R. S. Kane, Adv Mater, 2011, 23, 690-718.
82. K. W. Kolewe, K. M. Dobosz, T. Emrick, S. S. Nonnenmann and J. D. Schiffman, ACS applied bio materials, 2018, 1, 33-41.
83. Y. Zhu, J. Zhang, J. Yang, C. Pan, T. Xu and L. Zhang, J. Mater. Chem. B, 2016, 4, 5105-5111.
84. M. Wang and T. Tang, Journal of orthopaedic translation, 2018, 17, 42-54.
85. E. Ostuni, R. G. Chapman, M. N. Liang, G. Meluleni, G. Pier, D. E. Ingber and G. M. Whitesides, Langmuir : the ACS journal of surfaces and colloids, 2001, 17, 6336-6343.
86. G. Cheng, Z. Zhang, S. Chen, J. D. Bryers and S. Jiang, Biomaterials, 2007, 28, 4192-4199.
87. K. D. Park, Y. S. Kim, D. K. Han, Y. H. Kim, E. H. Lee, H. Suh and K. S. Choi, Biomaterials, 1998, 19, 851-859.
88. F. Oliveira, C. A. Lima, S. Brás, Â. França and N. Cerca, FEMS Microbiol. Lett., 2015, 362.

View Article Online
DOI: 10.1039/D5TB02919H

- Data for this article are available at the University of Illinois Chicago INDIGO data repository at https://researchguides.uic.edu/indigo/data.